DEVELOPMENT AND REVIEW OF THE IHRA (JARI) AND TNO PEDESTRIAN MODELS

M S Neale, B J Hardy and G J L Lawrence
TRL Limited
United Kingdom
Paper Number 499

ABSTRACT

This report details a project to review and develop the JARI pedestrian model as chosen by the IHRA to develop their pedestrian head impact test procedure. In the work several modifications were made to the model, including the removal of duplicated contacts defined between the model's arms and legs, modifications to allow axial stretching in the spine, and the implementation of shoulder joints. To test the biofidelity of the simulated shoulder joints predictions from the original and modified versions of the JARI model, in addition to those from a pedestrian model developed by TNO, were compared against the results from shoulder impact studies completed on PMHS's. It was found that all the models demonstrated very poor shoulder biofidelity. Furthermore, for the same simulated vehicle-pedestrian impacts, differences in the predicted head impact velocities and head impact angles from all the pedestrian models were as high as 3.9 $m.s^{-1}$ and 17.1° respectively.

INTRODUCTION

The International Harmonised Research Activities (IHRA) Pedestrian Safety Working Group is in the process of developing a sub-system head impact test procedure for assessing the aggressiveness of vehicle fronts to pedestrian head impacts. It has been decided that many details of the head impact test procedure will be based on the predictions from a pedestrian model simulating full-scale vehicle-pedestrian accidents. The predictions from the model will be used to relate the sub-system head impact test conditions to the head impact conditions in vehicle-pedestrian accidents. To obtain an understanding of the confidence that could be placed in the results of simplified multi-body pedestrian simulations the IHRA Pedestrian Working Group used three MADYMO pedestrian models to simulate a matrix of vehicle shapes and impact velocities. Under the same impact conditions each model was found to predict significantly different head impact conditions. Following a review of the predictions from the three pedestrian models the IHRA Pedestrian Working Group decided to further improve the most promising model, as developed by the Japan Automobile Research Institute (JARI). The improved model could then be used to refine the provisional test conditions in the IHRA head impact test procedure. However, although the JARI model suffered fewer obvious problems than the two other models reviewed, inconsistencies were discovered in its predictions, raising concerns on the model's biofidelic response and accuracy. The main concerns of the model's predictive capabilities related mainly to the biofidelity of the model's shoulder which is anticipated to have an important influence on the impact severity of the head with the vehicle front in vehicle-pedestrian impacts (IHRA Pedestrian Safety Working Group, 2001).

To address this concern, TRL Limited has undertaken a study funded by the UK Department for Transport (DfT) to review and develop the JARI pedestrian model. This paper details the findings from this work. It reports on the improvements made to the biofidelic structure of the original JARI model to enhance its predictive capabilities. The report details the differences in the original and improved model's predictions and additionally assesses the performance of a pedestrian model developed by TNO that could be used as an alternative model for developing the IHRA pedestrian head impact test procedure.

THE JARI PEDESTRIAN MODEL

Following a review of three MADYMO pedestrian models the IHRA Pedestrian Working Group decided to further improve the most promising model as developed by the Japan Automobile Research Institute (JARI) for use in the development of their sub-system head impact test procedure. A copy of this model was donated by JARI to TRL for the purposes of this investigation.

Structure of the JARI pedestrian model

Figure 1 shows the structure of the JARI pedestrian model. The model represents a 50^{th} percentile male pedestrian and is formed from 27 anatomical segments joined by a series of kinematic joints. With the exception of the elbows, the segments of the model are joined by a series of spherical or 'ball-and-socket' type joints. The elbows are formed from revolute or 'hinge' type joints. All the joints have a defined stiffness characteristic to approximate the stiffness and range of motion of the equivalent anatomical joint. In addition to the regular anatomical joints such as the knees and elbows, further joints have been implemented in the model to simulate the bending response of the long bones in the legs and arms.

In addition to the JARI pedestrian model, the Road Accident Research Unit (RARU) of Australia and TNO Automotive UK donated further MADYMO pedestrian models for the investigation. The RARU pedestrian model was one of the three models included in the original model review completed by the IHRA. It was known that this model possessed some superior features to the JARI pedestrian model and it was anticipated that these features could be transferred into the JARI pedestrian model to improve the biofidelity of its response.

The TNO pedestrian model (version release 2.2.1.2) was known to possess a more detailed structure than the JARI pedestrian model. Due to its enhanced structure it was anticipated that the TNO model predictions may be more accurate than those of the JARI pedestrian model and could possibly offer an alternative and better model for developing the IHRA sub-system head impact test procedure. It was therefore decided to include this model in the study in order to test the JARI pedestrian model's predictions against those of the TNO model. An illustration of this model is included in Figure 1. With the exception of some initial confirmation runs all the pedestrian models investigated in the study were run under the version 5.4 release of MADYMO.

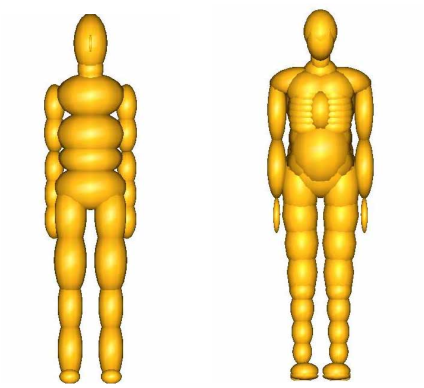

(a) **(b)**

Figure 1. The JARI (a) and TNO (b) pedestrian models.

INITIAL REVIEW OF THE JARI PEDESTRIAN MODEL

An initial review of the JARI model was completed to identify possible limitations that could affect the accuracy of its predictions. In addition, a brief review of the TNO pedestrian model was completed to compare the complexity of this model with the JARI model. Both the construction and animation outputs of the two models were examined and many general observations were made. The main ones of these were as follows:

- All anatomical segments in the JARI model are connected with rigid kinematic joints allowing at the most only 3-degrees of relative motion between the anatomical segments. In contrast, the TNO model has more complex joints in critical areas of the model's anatomy such as in the knees, neck and ribs, which allow a greater and more biofidelic range of movement between anatomical segments.
- The JARI pedestrian model has no shoulder joints, but shoulder joints have been simulated in the TNO model.
- The exterior profile of the TNO model more closely resembles that of a real pedestrian than the JARI model, as shown in Figure 1. It is expected that the improved exterior profile of the TNO model will promote better contact definition during simulated vehicle-pedestrian impacts and improve the accuracy of the TNO model's predicted pedestrian kinematics.
- During simulated vehicle-pedestrian impacts it was noticeable that there seemed to be a lack of rotation in the upper body of the JARI model, which could be anticipated in real vehicle-pedestrian impacts. Irregular rotations were also observed in the legs of the JARI model and large oscillatory motions were noticed in the model's abdomen, though this generally only occurred after head strikes with the simulated vehicle. In general the kinematics of the TNO model were more believable than those of the JARI model (i.e. no irregular rotations or oscillations of anatomical segments). However, the author's interpretation of the TNO model response is possibly influenced by it looking more like a real pedestrian than the JARI model.

MODIFICATIONS TO THE JARI PEDESTRIAN MODEL

The structure of the JARI and RARU pedestrian models were compared to identify critical features that could be taken from the RARU model and implemented in the JARI pedestrian model in order to improve its biofidelity. An isolated examination of the JARI model was also completed to check that there were no obvious limitations in its construction. From these investigations several modifications to the JARI pedestrian model were decided upon based on those that would potentially have the greatest improvement on the biofidelic behaviour of the model and more importantly the head impact response during simulated vehicle-pedestrian impacts.

Modification 1 - Removal of secondary contact between the arms and legs of the JARI pedestrian model

It was found during investigations of the JARI pedestrian model that the original model developers had inadvertently duplicated the contact definition between the arms and between the legs. This would lead to double the contact force being generated between the legs and between the arms when contacting each other during simulated vehicle-pedestrian impacts. Consequently, these duplicated contacts were removed.

Modification 2 – Introduction of spine axial translational joints

Rigid kinematic spherical joints were used to connect the anatomical segments of the JARI pedestrian model's torso to simulate the range of flexion in the spine. A limitation of these connections is that they prevent axial stretching of the spine, which can be considerable during vehicle-pedestrian impacts. In the RARU pedestrian model translational joints acting along the length of the spine have been introduced allowing the spine to stretch when loaded sufficiently. It was felt that the stretching response of the spine could have a considerable influence on the impact behaviour of the head. Consequently, the decision was made to introduce these translational joints into the spine of the JARI pedestrian model. Stiffness characteristics for both translational joints were the same and these were taken from the RARU pedestrian model.

Modification 3 - Introduction of shoulder joints

During vehicle-pedestrian impacts the leading shoulder can strike the vehicle structure prior to the head and thus influence the severity of the head impact with the vehicle front. Due to the shoulder's potential influence on the impact behaviour of the head it was considered important to accurately simulate the dynamic response of the shoulders in the JARI pedestrian model. It was discovered in investigations of the JARI model that the motion of the shoulders was not simulated. The assumption was made in the model's original construction that the shoulders were rigidly connected to the upper torso, although spherical joints did allow abduction, adduction, flexion, extension and rotation of the arms. It was anticipated that this set-up would potentially increase the protection offered by the shoulder to the head during simulated vehicle-pedestrian impacts.

The RARU pedestrian model possesses additional planar type joints that simulate the typical range of movement observed in the shoulders. These planar joints allow connecting bodies to displace relative to each other along a defined plane and also to rotate relative to each other about an axis perpendicular to the defined plane. Hence, the shoulder joints as implemented in the RARU pedestrian model possess three degrees of motion; two translational degrees of movement (i.e. anterior-posterior and vertical shoulder movement) and rotational movement of the shoulder about an axis perpendicular to the plane defined by the anterior-posterior and vertical axes of the shoulder. Consequently, the details of these shoulder joints were implemented in the JARI pedestrian model. Stiffness characteristics for the joints were also taken from the RARU model.

VALIDATION OF THE PEDESTRIAN MODELS

Several types of model validation runs were completed following the modifications made to the JARI pedestrian model. The first of these compared predictions from the original and modified versions of the JARI pedestrian models against measured kinematic data from full-scale post mortem human surrogate (PMHS) pedestrian impact tests provided by JARI. Next, for a series of simulated vehicle-pedestrian impacts, the predicted head impact behaviour from the original and modified JARI pedestrian models and the TNO model were compared. This was completed to assess the implications that there might be in using the JARI model for developing the IHRA sub-system head impact test procedure. Finally, the performance of the shoulder joints added to the JARI model were tested by comparing the original and modified JARI pedestrian model's predictions against measured data from PMHS shoulder impact studies completed by Bolte *et al.* (2000). The shoulder response of the TNO pedestrian model was also tested in this part of the validation to assess how its shoulder response compared with that of the original and modified versions of the JARI pedestrian model.

Validation 1 - Kinematics of the JARI pedestrian model

Predictions from the original and modified versions of the JARI pedestrian model were compared against body segment trajectory corridors and relative head impact velocities obtained from full-scale pedestrian PMHS impact tests involving two vehicle shapes; CAR A and CAR B. The dimensions of these vehicle fronts were supplied to TRL by JARI and these are detailed in **Table 1**. The initial speed of the vehicles in the tests was 40 $km.h^{-1}$ with a braking rate of 0.5 g.

The posture of the original and modified versions of the JARI pedestrian model were modified to match the set up of the PMHS's pre-impact. This involved having the model's arms folded in front of the torso and the right leg (leading leg) was placed slightly ahead of the left. Figure 2 shows the set-up of the original JARI pedestrian model for the CAR A simulated vehicle-pedestrian impact. The figure also shows the modelled vehicle structure used in the simulations. The design of the simulated vehicle front was provided in the original pedestrian model supplied to TRL by JARI. It is constructed from three cylinders defining the edges of the bumper, bonnet and lower limit of the vehicle front. Planes have been joined between these cylinders to form the skart, bumper, bonnet and windscreen of the simulated vehicle. These geometric shapes were re-positioned and re-sized to obtain the desired vehicle shapes for the simulated vehicle-pedestrian impacts. The impact stiffness of both CAR A and CAR B were the same and these details were also supplied by JARI. The simulated friction between the soles of the feet and ground was set at 0.67 and that between the pedestrian dummy and the vehicle front was set at 0.3.

Table 1
Simulated vehicle front dimensions of CAR A and CAR B

Vehicle dimension	CAR A	CAR B
Bumper lead (mm)	145	141
Bumper centre height (mm)	383	446
Bonnet leading edge height (mm)	763	641
Bonnet length (mm)	1124	1019
Bonnet angle (°)	6.8	8.8
Windscreen angle (°)	45.0	35.0

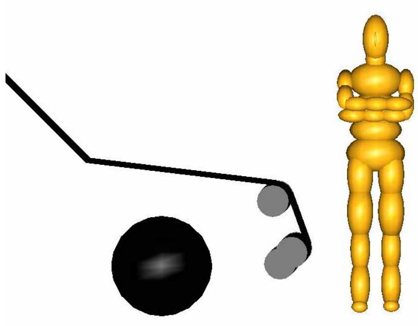

Figure 2. Set-up of the original JARI pedestrian model for the CAR A simulated vehicle-pedestrian impact.

Validation 2 - Comparison of predicted head impact velocities and head impact angles

Further simulated vehicle-pedestrian impacts were completed to compare predicted head impact velocities and head impact angles over a greater range of vehicle shapes. Two further vehicle shapes were investigated representing the profiles of a mid-sized Sedan and a mid-sized SUV. **Table 2** details the front geometry of these two additional vehicles. The simulated design and stiffness of the vehicle fronts matched that of the simulated CAR A and CAR B vehicle fronts. The initial impact speed and braking acceleration of the simulated vehicles were 40 $km.h^{-1}$ and 0.5g respectively. However, for these runs the posture of the pedestrian models was altered to a more natural walking stance. The simulated friction between the soles of the feet and ground was set at 0.67 and that between the pedestrian dummy and the vehicle front was set at 0.3.

For the two vehicle shapes in **Table 2**, simulated vehicle-pedestrian impacts were also completed with the TNO pedestrian model in addition to the original and modified JARI pedestrian models. These additional simulations were completed to test the performance of the JARI versions of the pedestrian model against that of the TNO model. Also included in the comparisons made were the predicted head impact velocities and head impact angles obtained from the original and modified JARI pedestrian models for the CAR A and CAR B simulated impacts.

Table 2.
Front profiles of the simulated mid-sized Sedan and mid-sized SUV vehicles

Vehicle dimension	Sedan	SUV
Bumper lead (mm)	127	127
Bumper centre height (mm)	475	516
Bonnet leading edge height (mm)	702	839
Bonnet length (mm)	917	635
Bonnet angle (°)	14	18
Windscreen angle (°)	34	40

Validation 3 – Biofidelity of the JARI and TNO modelled shoulder joints

Bolte *et al.* (2000) conducted a series of impact studies on seated PMHS's to assess the behaviour and threshold injury response of the shoulder to lateral impacts. In this work eleven non-embalmed human PMHS's were successively impacted on the left and right shoulders with a 23 kg pneumatic ram at the level of the glenohumeral joint. All the PMHS's used in the study were received and tested less than 48 hours post mortem. These were instrumented with ten tri-axial accelerometers, located at the sternum, first thoracic vertebra, right and left acromion processes, the lateral and medial thirds of each clavicle and on each scapula. The impacting surface of the ram was 20.32 cm by 15.24 cm and the ram was covered with a 5.08 cm thick piece of Arcel 310, 26.4 kg.m^{-3} density foam padding. For the impact tests the initial impact speed of the ram was tuned to values between 3.5 and 7.0 m.s^{-1} in order to achieve a threshold impact severity on the impacted shoulder.

The original and modified versions of the JARI pedestrian model and the TNO pedestrian model were modified to match the set-up of Bolte's experiments. Limited details were available concerning the set-up of the PMHS's for the tests and many of these were estimated in the models. These included details on the exact seating posture of the PMHS's and the geometry and structure of the bench that the PMHS's were seated on for the impact tests.

It was not possible to obtain details on the stiffness characteristics of the Arcel foam added to the front of the impacting ram. Initially the simulated stiffness characteristics for this material were matched to data obtained from impact tests conducted on motorcycle helmet liners, which was anticipated to exhibit a similar impact behaviour to the Arcel foam. However, predicted shoulder impact forces using these material characteristics were very different from those measured and it was uncertain if the differences were due to limitations of the pedestrian models or a consequence of incorrect stiffness characteristics being defined for the impacting ram. To resolve this problem the stiffness characteristics of the simulated ram were modified so that the predicted shoulder impact force on the pedestrian models was similar in magnitude and profile to those measured. Although this effectively fixed the impact behaviour of the simulated impacts it was rationalised that any further differences observed between predicted and measured responses could be attributed solely to limitations in the pedestrian models.

In order to compare their measurements, Bolte *et al*. (2000) normalised their results to that of a fiftieth percentile male and separated and presented their results according to three impact severities of the ram. The three impact severities were 3.7-4.2, 4.2-4.75 and 5.0-7.0 m.s^{-1} as defined by the ram's initial impact velocity. Consequently, initial ram velocities of 3.95, 4.48 and 6.00 m.s^{-1} were simulated in the shoulder impacts on the pedestrian models.

VALIDATION RESULTS

Results - Kinematics of the JARI pedestrian model

Figures 3 and 4 provide a typical example of the results obtained from the kinematic validations of the JARI pedestrian model. In general it was found that the predicted body segment trajectories and head impact velocities of the original and modified versions of the JARI model are very similar. It is suggested from these results that the modifications made to the JARI model have had a limited influence on the accuracy of these predictions from the model.

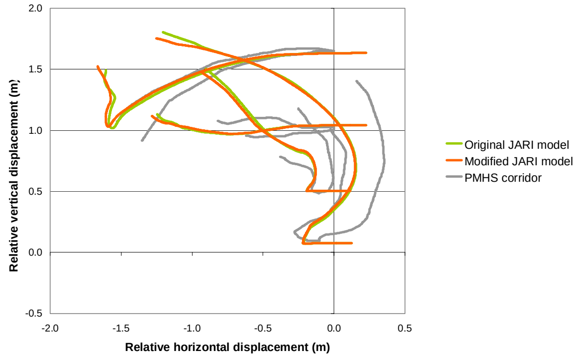

Figure 3. Predicted body segment trajectories and PMHS corridors for the CAR A impacts.

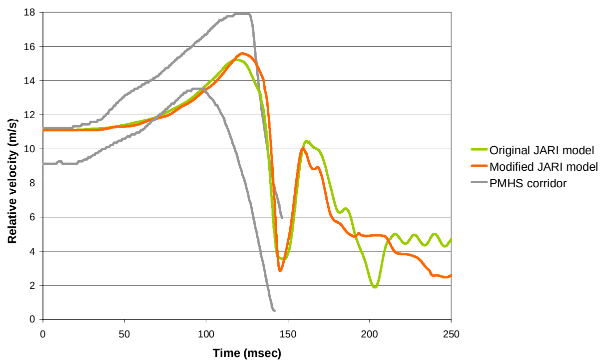

Figure 4. Predicted relative head velocities and PMHS corridors for the CAR A impacts.

Results – Comparison of predicted head impact velocities and head impact angles

Predicted body segment trajectories from the two versions of the JARI model were compared against equivalent predictions from the TNO pedestrian model for simulated impacts into a mid-sized Sedan and mid sized SUV. Figure 5, which contains the predicted body segment trajectories for the mid-sized Sedan impacts shows that the profiles of the predicted trajectories are very similar though the deviation in the TNO model's predictions from those of the JARI models is greater later on in the impact. In contrast, the profiles of the TNO predicted trajectories for the mid-sized SUV impact (Figure 6) are very different from those predicted by the JARI models.

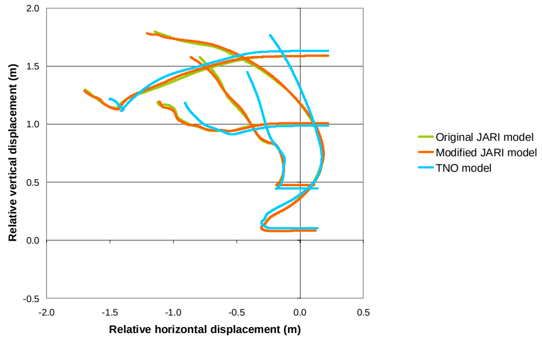

Figure 5. Comparison of predicted body segment trajectories for the mid-sized Sedan simulated impacts.

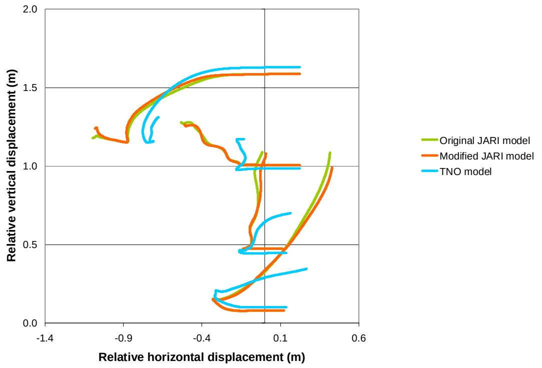

Figure 6. Comparison of predicted body segment trajectories for the mid-sized SUV simulated impacts.

Predicted head impact velocity relative to the vehicle front. Figures 7 and 8 compare the predicted relative head velocity-time history responses for the mid-sized Sedan and SUV pedestrian impacts respectively. The largest difference is observed in the predicted relative head velocities for the Sedan impact where the peak relative head velocity predicted by the TNO pedestrian model is around 2 $m.s^{-1}$ greater than that predicted by either the original or modified versions of the JARI pedestrian model. In contrast to these results, the predicted relative head velocities for the SUV pedestrian impacts are very similar. The difference between the predicted TNO peak relative head velocity and that of the JARI pedestrian models is less than 1$m.s^{-1}$.

Table 3 details the relative head impact velocities predicted by the original and modified JARI pedestrian models and the TNO pedestrian model for the simulated impacts into the mid-sized Sedan and SUV. The Table also includes the relative head impact velocities obtained from the original and modified JARI simulated impacts into CAR A and CAR B vehicle fronts. These results show that none of the models consistently predict either the highest or lowest relative head impact velocities. The lowest predicted head impact velocity is provided by the TNO model for the mid-sized SUV simulation and the highest is produced by the modified JARI model for the CAR A simulation. The largest difference in the model predictions is obtained for the mid-sized Sedan simulation where the difference is 3.66 $m.s^{-1}$.

Table 3.
Predicted relative head impact velocities for the pedestrian models impacted at 11.11 $m.s^{-1}$

Vehicle Type	Predicted head impact velocity ($m.s^{-1}$)		
	Original JARI model	Modified JARI model	TNO model
CAR A	13.16	14.02	Not simulated
CAR B	13.27	12.66	Not simulated
Mid-sized Sedan	9.98	10.48	13.64
Mid-sized SUV	9.79	10.12	8.89

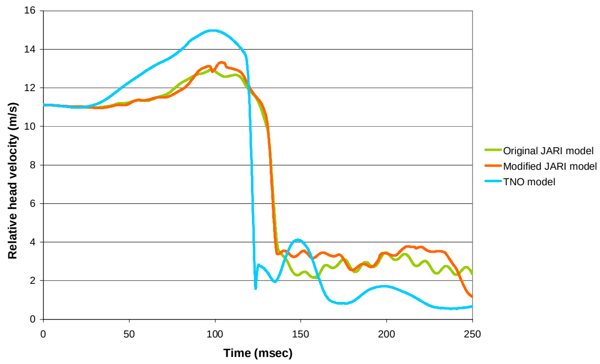

Figure 7. Comparison of predicted relative head velocities for the mid-sized Sedan simulated impacts.

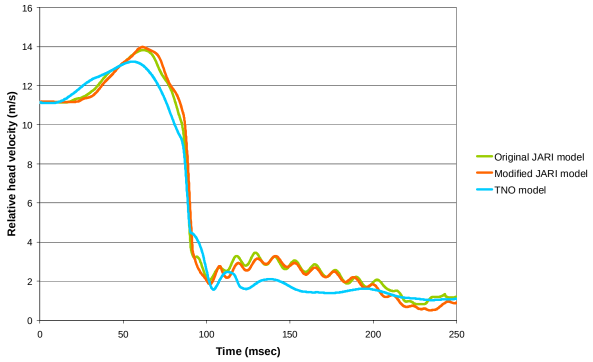

Figure 8. Comparison of predicted relative head velocities for the mid-sized SUV simulated impacts.

Predicted head impact angles relative to the vehicle front. Predicted head impact angles for the simulated vehicle-pedestrian impacts were determined using the following formula;

Head Impact Angle = arctan (V_{RX}/V_{RZ})

Where;

V_{RX} = Head horizontal impact speed relative to the vehicle at time of vehicle-head impact;

V_{RZ} = Head vertical impact speed relative to the vehicle at time of vehicle-head impact.

Table 4 details the relative head impact angles predicted by the original and modified JARI pedestrian models and the TNO pedestrian model for the simulated impacts into the mid-sized Sedan and SUV. The Table also includes the relative head impact angles obtained from the original and modified JARI simulated impacts into CAR A and CAR B vehicle fronts. As with the predicted head impact velocities none of the models was found to consistently predict either the highest or lowest head impact angles. The largest difference in the results was for the mid-sized SUV simulation in which the original JARI pedestrian model predicted a head impact angle 17° larger than that predicted by the TNO pedestrian model.

Table 4.
Predicted relative head impact angles for the pedestrian models impacted at 11.11 m.s^{-1}

Vehicle Type	Predicted head impact angle (°)		
	Original JARI model	Modified JARI model	TNO model
CAR A	103	98	Not simulated
CAR B	70	76	Not simulated
Mid-sized Sedan	84	93	86
Mid-sized SUV	107	104	90

Results – Biofidelity of the JARI and TNO modelled shoulder joints

Predictions from the two versions of the JARI model and the TNO model were compared against the measured responses obtained by Bolte *et al*. (2000). These included comparisons of the force-time histories of the impacts, estimated effective masses of the impact and the relative shoulder displacement as defined by the acromion-sternum displacement.

Comparison of measured and predicted force time histories. Predicted impact forces from the model runs were compared against samples of the normalised impact force responses produced by Bolte *et al*. (2000). As in the results of Bolte these were grouped within defined velocity ranges that the impact ram struck the PMHS's in test. Figure 9 provides an example of the results obtained. It shows that the magnitude and period of the predicted responses broadly match the measured responses. This result could be expected given that the simulated stiffness of the impacting ram was modified to get the predicted impact forces to match those measured.

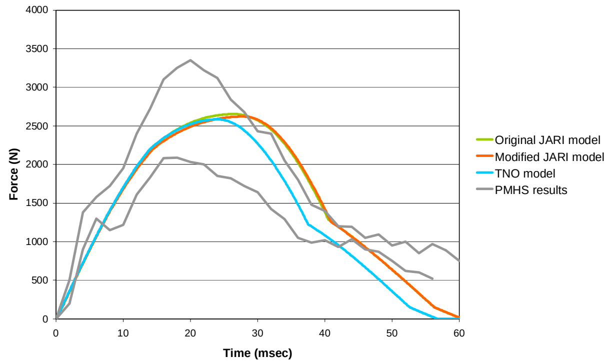

Figure 9. Predicted and measured normalised force time histories for shoulder impacts between 3.7-4.2 m.s^{-1}.

Comparison of measured and predicted effective masses. The measured effective impact mass for the PMHS shoulders was estimated by dividing the impulse of the shoulder impact by the change in velocity of the first thoracic vertebra. The change in thoracic vertebra velocity was determined from the time of initial contact until the time when the impacted acromion was maximally displaced with respect to the non-impacted acromion. The shoulder impacts resulted in fractured and non-fractured impacts to the shoulders. The average estimated effective masses for the non-fractured, fractured and overall impacts were as follows:

- Average effective mass for non-fractured impacts 20.7 kg
- Average effective mass for fractured impacts 18.7 kg
- Overall effective mass of impacts 19.9 kg

Bolte also normalised their results and found that the average effective mass for the 50th percentile male was 24.0kg.

It was not possible to estimate effective impact masses for the pedestrian models according to the method used by Bolte as there was very little acromion-acromion displacement in the pedestrian models as detailed below. Consequently, effective shoulder impact masses for the pedestrian models were calculated by dividing twice the energy of the shoulder impact by the square of the velocity of the impacted acromion at the time of zero relative velocity between the ram and the impacted shoulder.

Effective impact shoulder masses were estimated for all three simulated ram impact speeds of 3.95, 4.48 and 6.00 m.s^{-1}. These results are detailed in **Table 5** and show that the predicted effective masses are at least 6 kg higher than that estimated for the 50th percentile shoulder impact. The lowest effective masses for the predicted responses were estimated for the TNO pedestrian model. These estimated effective masses were between 3.5 and 6.6 kg lower than those estimated for the original and modified JARI models depending on the ram impact velocity. Estimated effective masses for the modified JARI model were also consistently lower than those estimated for the original JARI model. The differences between the original and modified JARI model effective masses were between 0.4 and 3.0 kg.

Table 5
Estimated effective masses for the shoulder impacts

Ram impact velocity (m.s^{-1})	Effective mass (kg)			
	Original JARI model	Modified JARI model	TNO model	PMHS 50th % ile
3.95	36.9	33.9	30.2	24.0
4.48	37.8	35.2	31.7	
6.00	41.4	41.0	34.4	

Comparison of measured and predicted acromion-sternum displacement. Average measured acromion-sternum displacements for the non-fractured and fractured PMHS impacts were respectively 47.6 and 33.5mm. The overall average measured acromion-sternum displacement was 39.0 mm with a standard deviation of 22.0 mm.

Table 6 details the predicted acromion-sternum displacement for the simulated ram impacts to the shoulders of the three investigated pedestrian dummy models at the three initial ram impact speeds of 3.95, 4.48 and 6.00 m.s^{-1}. All these predicted displacements are considerably smaller than the measured responses. The original JARI model exhibits no displacement of the acromion-sternum for the impacts and only minor displacements are observed in the modified JARI model. In comparison to the predicted displacements from the original and modified JARI models those predicted by the TNO pedestrian model are much larger, averaging around 3.68 mm. However, even the predicted acromion-sternum displacements of the TNO model were on average ten times smaller than those measured.

Table 6
Acromion-sternum displacement for the shoulder impacts

Ram Impact velocity (m.s^{-1})	Acromion-sternum displacement (mm)			
	Original JARI model	Modified JARI model	TNO model	Average PMHS measured response
3.95	0.000	0.003	3.171	39.0
4.48	0.000	0.003	3.492	
6.00	0.000	0.004	4.373	

DISCUSSION

The principal objective of this study was to improve the biofidelic response of the JARI pedestrian model in order to alleviate concerns that exist in applying the model for developing the IHRA Pedestrian Working Group's head impact test procedure. To fulfil this role it is essential that the JARI model is able to accurately predict the impact behaviour of the head during simulated vehicle-pedestrian impacts. Despite modifications made to the JARI model in this study it is uncertain if the accuracy of the predicted impact behaviour of the JARI modelled head has been improved.

Simulated shoulder response

The action of the shoulder is considered to have a critical influence on the impact behaviour of the head with the vehicle front during vehicle-pedestrian impacts. It was identified prior to this study that the simulated shoulder was one of the main limitations in the biofidelity of the JARI pedestrian model and modifications were made in this study to address this issue. When compared against test results from shoulder impacts of PMHS published by Bolte *et al.* (2000) it was found that the modified JARI model provided a consistent, but only slightly better biofidelic shoulder response than the original JARI model. Overall, both versions of the JARI model provided poor biofidelic shoulder responses in comparison to the measured PMHS test data.

Predictions from the TNO pedestrian model were also included in these comparisons to determine if this model provided a better biofidelic shoulder response than the JARI model. In comparison to the predictions from the two versions of the JARI model the TNO model did provide an overall better biofidelic response. Predicted effective masses and acromion-sternum displacements from the TNO model correlated more closely with the measured PMHS data than the JARI model. However, as with the JARI model the TNO model was also considered to provide a poor biofidelic shoulder response. Predicted effective masses from all the pedestrian models were on average 6 kg higher than those estimated from the test results and the best predicted acromion-sternum displacements as provided by the TNO model were on average ten times smaller (36 mm lower) than those measured.

The poor biofidelity in the simulated shoulder responses raises concerns on the accuracy to which the models can predict the impact behaviour of the head given the anticipated influence that the shoulder has on the head impact response during vehicle-pedestrian accidents. In general the shoulder impact comparisons indicate that the simulated shoulder responses are too stiff in comparison to that of real shoulders loaded under severe impact conditions. The differences in the predicted and measured shoulder response can be attributed to a number of limitations in the models' structures, which can be resolved given the necessary resources.

Limitations of the simulated shoulder structure

The structure of the shoulders in both the modified JARI and TNO pedestrian models adequately simulate the normal degrees of movement in the shoulder joint. However, it is noticed in the comparisons against PMHS test data that large differences exist in the simulated and measured shoulder responses under severe loading conditions. Severe impacts to the shoulder will result in abnormal deformations and compressions of the shoulder and upper torso that are not currently simulated in the pedestrian models. Severe impact loads to the shoulder will result in compression of the shoulder joint, bending and relative displacement of the bones forming the shoulder complex, compression of the rib cage and complex articulations, as well as shearing and stretching of the thoracic and cervical spine. It is anticipated that all these actions will contribute to the differences observed between measured and predicted shoulder behaviour.

It is recognised that further modifications to both the JARI and TNO models are needed to improve the biofidelity of the predicted shoulder response under severe shoulder impacts. This would help to improve the confidence in the models' predictions and especially the predicted impact behaviour of the head during simulated vehicle-pedestrian impacts.

Comparison of predicted head impact behaviour

It is uncertain how much an improved biofidelic shoulder response in the model's would influence the predicted head impact behaviour. Indications are that these might be considerable. For despite only minor differences in the biofidelity of the models' shoulder responses, more significant differences were observed in the predicted head impact behaviour from the original and modified JARI pedestrian models and the TNO pedestrian model. Simulated vehicle-pedestrian impacts were into bonnet leading edge heights ranging between 641 and 839 mm. For the equivalent simulated impacts into the same vehicle fronts the differences in the original and modified JARI predicted head impact velocities and head impact angles ranged between values of 0.3 – 0.9 $m.s^{-1}$ and 3.3 – 9.6° respectively. Greater differences were observed between the head responses predicted by the JARI and TNO models, where differences in the predicted head impact velocities and head impact angles for simulated impacts into the same vehicle fronts were as high as 3.9 $m.s^{-1}$ and 17.1° respectively. Similar differences in head impact behaviour would significantly alter the level of impact energy applied to a vehicle front for the purposes of sub-system testing for pedestrian head strikes. The accuracy of the JARI pedestrian model's predicted head behaviour is therefore imperative to the IHRA developing a representative sub-system head impact test procedure and a key element to achieving this is to improve the biofidelity of the model's shoulder response.

Although there are indications that improving the biofidelity of the model's shoulder response would have a considerable effect on the predicted head impact behaviour it is difficult to suggest if the improvements would result in lower or higher predicted head impact values. Examinations of the models' predictions found that none of the models consistently provided the highest or lowest predicted head impact angles and head impact velocities, even though consistent differences were observed in the biofidelity of their shoulder responses.

Predicted body segment trajectories

It was found in comparisons of predicted body segment trajectories and relative head impact velocities from the original and modified versions of the JARI pedestrian model that these results are very similar. Furthermore, both sets of predictions broadly matched equivalent measurements obtained from PMHS vehicle-pedestrian impacts as provided by JARI. Although several modifications were made to the JARI model, including the facilitation of a stretching response in the spine and the inclusion of shoulder joints in the model, these results suggest that the modifications made have had a limited influence on the general kinematic behaviour of the model. This result is consistent for all the vehicle profiles investigated in this study which had simulated bonnet leading edge heights of between 641 and 839 mm.

Predicted body segment trajectories from the TNO model were also similar to those predicted by the original and modified versions of the JARI model for simulated vehicle-pedestrian impacts into a relatively low profile mid-sized Sedan vehicle. Despite the large differences in the structure of the JARI and TNO pedestrian models the results from the comparisons would suggest that the structure of the models has a minor influence on the general kinematic behaviour of the models. However, the similarity between the models' predictions was found to be very dependent on the vehicle shapes used in the simulated vehicle-pedestrian impacts. For a higher profiled simulated SUV vehicle-pedestrian impact there were considerable differences between the body segment trajectories predicted by the TNO model and those predicted by the two versions of the JARI model, as shown in Figure 6. These differences are also highlighted in the animations of the simulated SUV vehicle-pedestrian impacts. Figure 10 shows animated frames from the original JARI simulation of the SUV vehicle-pedestrian impact. As shown in this figure, the pedestrian model slides onto the SUV vehicle bonnet during the model run. In contrast, Figure 11 shows that the TNO pedestrian model for the SUV model simulation tended to get pushed ahead of the vehicle front during the vehicle-pedestrian simulated impact.

The purpose of including the TNO pedestrian model in the study was to determine if it provided a better alternative pedestrian model for developing the IHRA pedestrian head impact test procedure than the JARI pedestrian model. None of the comparisons completed in this study provide any obvious indications of which model should be used. However, the gross differences in the general kinematics of the pedestrian models for the high sided SUV impact provides a useful separation of which model provides the most accurate pedestrian predictions. Comparing these model results against matching PMHS test data would help in the decisions of which model provides the most accurate predictions. However, PMHS data used in this study were for relatively low-sided vehicles where the body-segment trajectories of the different models were found to be similar. Further work is thus deemed necessary to validate the models' predictions over a larger range of vehicle shapes to determine if the TNO model provides a significant improvement in predictive accuracy over the JARI model.

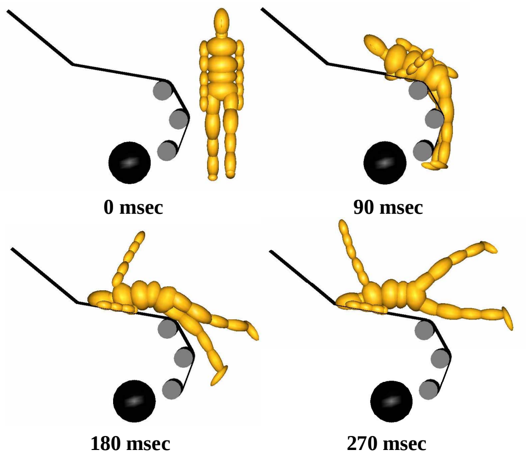

Figure 10. Animated frames of the original IHRA pedestrian model impact with the mid-sized SUV.

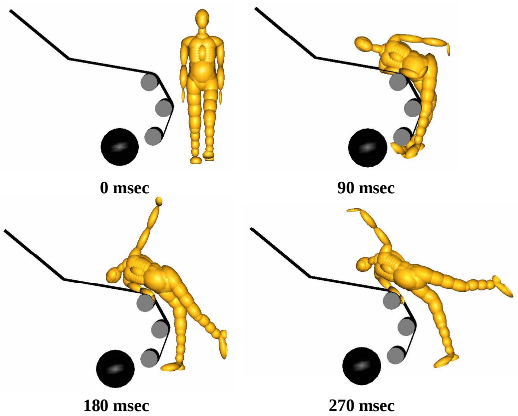

Figure 11. Animated frames of the TNO pedestrian model impact with the mid-sized SUV.

CONCLUSIONS

This work has aimed to improve the impact behaviour of the JARI pedestrian model's head during simulated vehicle-pedestrian impacts. Modifications made to the model to improve its biofidelity included the introduction of additional model joints to allow axial stretching of the spine and the development of shoulder joints for the model. Predictions from the original and modified versions of the JARI pedestrian model were then compared against measurements from full-scale vehicle-pedestrian impact tests and shoulder impact tests completed on PMHS's. The predictions from the two versions of the JARI pedestrian model were also compared against the predictions from an additional pedestrian model produced by TNO. The general conclusions that can be made from the work are as follows:

- The modified JARI pedestrian model was found to have slightly better shoulder biofidelity than the original JARI pedestrian model. The TNO shoulder was found to have slightly better biofidelity than either the original or modified versions of the JARI pedestrian model.
- In comparison to test data from PMHS shoulder impacts all the models demonstrated very poor shoulder biofidelity and all simulated responses were too stiff in comparison to PMHS shoulder responses. Predicted effective masses were 6 kg higher than those measured and the best predicted acromion-sternum displacements were on average ten times smaller (36 mm lower) than that measured.
- The poor biofidelity of the simulated shoulder responses is attributed to the pedestrian models not simulating abnormal compressions and deformations of the shoulder during severe impacts. This would include bending and relative displacement of the bones forming the shoulder complex, compression of the shoulder joint, compression and bending of the rib cage and complex articulations, shearing and stretching in the thoracic and cervical spine.
- Simulated vehicle-pedestrian impacts were into vehicle fronts with bonnet leading edge heights ranging between 641 and 839 mm. For simulated vehicle-pedestrian impacts into the same vehicle front the difference in the predicted head impact velocities and head impact angles from the original and modified JARI models ranged between values of 0.3 – 0.9 $m.s^{-1}$ and 3.3 – 9.6° respectively. The differences in the predicted head impact velocities and head impact angles from the JARI and TNO pedestrian models for simulated vehicle-pedestrian impacts into the same vehicle front were as high as 3.9 $m.s^{-1}$ and 17.1° respectively.
- Despite consistent differences in the shoulder biofidelity of the pedestrian models, none of the models consistently predicted either the highest or lowest head impact velocities and head impact angles. Consequently it is not possible to state if improving the biofidelity of the simulated shoulder will increase or reduce predicted head impact velocities and head impact angles.
- It is not possible to say from this work if the TNO model provides a superior model to the JARI model for developing the IHRA head impact test procedure. However, significant differences were observed in the TNO and JARI pedestrian models' kinematic behaviour for simulated impacts into a high profiled vehicle front with a bonnet leading edge height of 839 mm. It is suggested that the predictions from both pedestrian models should be validated against measured data from PMHS impact tests into high profiled vehicles in order to gauge which model provides the most accurate biofidelic response.

ACKNOWLEDGEMENTS

The work described in this report was carried out in the Biomechanics and Injury Prevention Group of TRL Limited and was funded by the UK Department for Transport. The authors are grateful to JARI for supplying copies of their model, background information and validation data against which the model's predictions were compared. Further gratitude is expressed to RARU and TNO for supplying additional pedestrian models for use in this investigation.

REFERENCES

Bolte J H, Hines M H, McFadden J D and Saul R A (2000). *Shoulder response characteristics and injury due to lateral glenohumeral joint impacts.* Proceedings of the 44th STAPP Car Crash Conference, Atlanta, Georgia, 6-8 November 2000, pp 261-280.

IHRA Pedestrian Safety Working Group (2001). *International Harmonized Research Activities Pedestrian Safety Working Group. 2001 report.* Document IHRA/PS/200. Tokyo, Japan: Japan Automobile Standards Internationalization Center. (Document available at http://www-ihra.nhtsa.dot.gov/)